An Atoms in Molecules and Electron Localization Function Computational Study on the Molecular Structure of the 6-Tricyclo[3.2.1.0^{2,4}]octyl Cation

Nick Henry Werstiuk* and Yi-Gui Wang

Department of Chemistry, McMaster University, Hamilton, Ontario,L8S 4M1, Canada

Received: July 11, 2001; In Final Form: October 22, 2001

The structure of 6-tricyclo[3.2.1.0^{2,4}]octyl cation **1** was optimized at HF, Becke3PW91, Becke3LYP, MP2, and MP2(full) levels with the 6-311G(d,p) basis set. Becke3PW91 and MP2(full) yielded similar values for the geometrical parameters of optimized **1**. When the C4−C6 distance was changed incrementally through the range 1.40−2.32 Å at the Becke3PW91/6-311G(d,p) level, there was no discontinuity in the total energy and the geometrical parameters of the cyclopropyl group underwent marked changes. AIM (the theory of atoms in molecules) and ELF (electron localization function) analyses were carried out to investigate the molecular structure of **1**. No bond path was found between C4 and C6 so **1** is a classical cation without pentacoordinated carbon atoms. Only when the C4−C6 distance was fixed in the range of 1.50−1.62 Å does **1** become a pentacoordinate (nonclassical) species in which C4 is connected to C2, C3, C5, C6, and H13 with bond paths. On the other hand, when the 6-tricyclo[3.2.1.0^{2,4}]octyl cation was substituted with Li and BeH groups at C4 and C5, the optimized equilibrium species exhibted pentacoordinate carbons at C4. Compared with the C1−C2 bond that we take as a normal single bond, the bonds between C4 and C2, C3, C5 are weak, as evidenced by reduced densities $\rho(\mathbf{r})$, significantly smaller $\nabla^2\rho(\mathbf{r})$ values, and large ellipticities at the bond critical points (BCPs). The delocalization indices (DIs)—the first application of a DI analysis in the study of carbocations—for these C−C bonds ranged between 0.733 and 0.860, smaller than unity. The DI between C4 and C6 is 0.634, suggesting that there is a significant degree of homoconjugation between C4 and C6. For polycyclic species such as **1**, it appears that a delocalization index of approximately 0.7 and an internuclear distance of 1.6 Å are required for a bond path to materialize between remote carbons. In an ELF analysis we found a small disynaptic basin V(C4,C6) between C4 and C6 that correlated with the existence of a (3, −1) critical point in $-\nabla^2\rho(\mathbf{r})$. The properties of ELF disynaptic basins around C4 and a contribution analysis showed a high degree of delocalization at this center.

Introduction

Acetolysis of the *exo,exo*-, *exo,endo*-, *endo,exo*-6-tricyclo-[3.2.1.0^{2,4}]octyl brosylates and nortricyclyl-3-carbinyl brosylate gives virtually identical mixtures of three acetates. A big difference in the solvolytic rates for the *exo,exo*-, and *exo,endo*-6-tricyclo[3.2.1.0^{2,4}]octyl brosylates led researchers to conclude that the 6-tricyclo[3.2.1.0^{2,4}]octyl cation (**1**) is a so-called nonclassical species even though the *exo,exo*-6-tricyclo[3.2.1.0^{2,4}]-octyl brosylate is less reactive by a factor of 0.15 than *exo*-2-norbornyl brosylate.[1,2] We have studied the 6-tricyclo[3.2.1.0^{2,4}]-octyl cation potential energy (PE) surface computationally and established that **1** is one of three common intermediates in the acetolysis of the brosylates and its molecular structure and rearrangement are important in determining the product compositions, the product distributions and the optical purities of the products.[3] The cyclopropyl group has long been considered to be similar to a double bond and so can stabilize cations even at remote positions.[4] It has played an important role in the development of the concept of homoaromaticity.[5] The molecular structure of **1** is intriguing because a number of representations shown as **1a**−**1e**[2,4] were considered as possibilities for its molecular structure clearly indicating that there was some confusion about how to describe its bonding. If bond critical points can be located for the dashed bonds between C4 and C6 with AIM (the theory of atoms in molecules), then **1** can be considered a nonclassical species because C4 is pentacoordinate

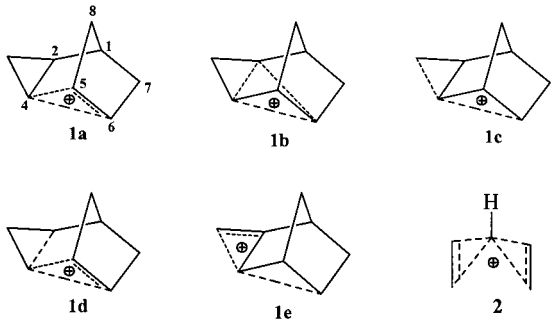

in these cases. Species **1a**, **1c**, **1d**, and **1e** can be viewed as unsymmetrical derivatives of pentacoordinate cation **2**, one of the species on the $C_5H_9^+$ PE surface.[6,7] On the other hand, it is possible that **1** is a π/π or σ/π no-bond homoconjugated species in which there is no bond path between C4 and C6.[5]

We showed in our previous publications that topologically based AIM and ELF (electron localization function) analyses are the methods of choice for studying so-called "nonclassical" species.[8−11] In AIM, molecular space is partitioned through an analysis of the gradient vector field of the one-electron density $\rho(\mathbf{r})$ and a bond path is a line of maximum electron density between two nuclei. Any lateral displacement from this line leads to a decrease in $\rho(\mathbf{r})$.[12,13] Two nuclei are considered to be bonded when linked by a bond path. The integration of the one-electron density within an atomic basin gives the atomic electron

10.1021/jp012642u CCC: $20.00
Published on Web 11/30/2001

TABLE 1: Selected Internuclear Distances (Å) of Cation 1 Optimized at Various Levels with the 6-311G(d,p) Basis Set

level of theory	C1−C2	C2−C3	C2−C4	C3−C4	C4−C5	C4−C6	C5−C6
HF	1.530	1.409	1.637	1.645	1.555	1.692	1.442
Becke3LYP	1.538	1.427	1.623	1.644	1.566	1.726	1.453
Becke3PW91	1.531	1.424	1.618	1.634	1.559	1.697	1.451
MP2	1.530	1.431	1.616	1.645	1.562	1.690	1.458
MP2(full)	1.528	1.430	1.613	1.642	1.560	1.686	1.456

population, and consequently the net atomic charge. On the other hand, integration of the pair density within a single basin and between two basins will separately yield the localization index $\lambda(A,A) = |F(A,A)|$ and the delocalization index $\delta(A,B) = |F(A,B)| + |F(B,A)|$.[14−16]

The other method we used involved a topological analysis of the gradient vector field of the Becke−Edgecombe electron localization function (ELF)[17] as implemented by Silvi and coworkers.[18] In ELF, core basins are organized around nuclei (with $Z > 2$), providing an inner-atomic shell-like structure and valence basins occupy the remaining space. In the ELF picture, bonding is defined on the basis of how valence basins interact with core basins, that is the number of core basins a valence basin is stuck on.[19] Numerous applications of ELF have demonstrated that a number of key points can be considered. A small basin population and a large basin fluctuation λ (>0.5) indicates a high delocalization, and the contribution analysis can show how basins are delocalized.[20] While there is usually a disynaptic basin between two bonded atoms, it has been suggested that "ionic" bonding is indicated if a basin is close to the core region of one of the atoms and no longer on the connection line.[21] We have studied **1** with AIM and ELF and computed delocalization indexes (DIs)—the first application of DIs to the study of carbocations—with the goal of gaining information on the nature of the bonding at the C4−C5−C6 face of **1** and thereby establishing whether it is, in fact, best described as a pentacoordinate nonclassical species. Our findings and analyses are documented in this paper.

Computational Details

Hartree−Fock (HF), DFT (Becke3PW91, Becke3LYP), and MP2 calculations were carried out with Gaussian94[22] on SGI Octane and SGI 2001 computers and with Gaussian98[23] on a Cray T90. The Becke3PW91/6-311G(d,p) level of theory was employed to obtain optimized geometries (Table 1) and wave functions throughout. As we established previously, calculations with the Becke3PW91 functional yielded geometries close to those obtained at the MP2(full) level with the same basis sets.[11] Frequency calculations at the Becke3PW91/6-311G(d,p) level confirmed that cations **1-opt**, **3-opt**, and **4-opt** are minimum on the potential energy surface. The total energies in Table 2 (Supporting Information) do not include zero-point energies. At any rate, whether zero-point energies are included in studies of this type does not impact on the topological analyses. The studies of the electron density $\rho(\mathbf{r})$, its gradient vector field $\nabla\rho(\mathbf{r})$, and its Laplacian $\nabla^2\rho(\mathbf{r})$, as well as the integrations, were carried out with the AIMPAC suite of programs[24] with the appropriate wave function. Electronic charge is locally concentrated in regions where $\nabla^2\rho(\mathbf{r}) < 0$. In the text, $L(\mathbf{r})$ refers to $-\nabla^2\rho(\mathbf{r})$ not $-\nabla^2\rho(\mathbf{r})/4$. We used the AIMDELOC program[25] to calculate the localization ($\lambda(A,A)$) and delocalization indexes ($\delta(A,B)$) based on the Becke3PW91/6-311G(d,p) overlap matrix of each atom obtained from the AIMPAC integrations. We also obtained the LIs and DIs at the HF/6-311G(d,p)//Becke3PW91/6-311G(d,p) and HF/6-311G(d,p)//HF/6-311G(d,p) levels to establish how the DFT and HF LIs and DIs compare. The DFT and HF results are virtually identical with the same basis set (Table 5). The ELF study was carried out with Silvi's TopMod package.[26,27] A box size that extended 3.0 au from the outermost atomic coordinates in each direction and a step size of 0.1 au were typically used in these calculations. Additional details on the ELF calculations can be found in ref 11. The results were visualized with SciAn.[28]

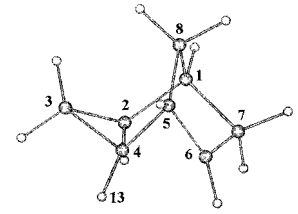

1-opt

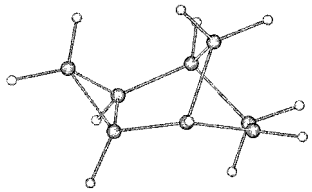

3-opt

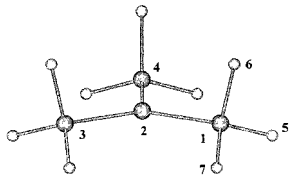

4-opt

Results and Discussion

Energy and Geometry of the *exo*-6-Tricyclo[3.2.1.0^{2,4}]octyl Cation as a Function of the C4−C6 Distance. HF, Becke3PW91, Becke3LYP, MP2, and MP2(full) calculations (with the 6-311G(d,p) basis set) yielded similar values for the geometrical parameters for optimized **1**. At the Becke3LYP/6-311G(d,p) level, the crucial C4−C6 distance (Table 1) was 1.726 Å, 0.03 Å longer than the average distance found with the other levels of theory. Unless specified otherwise, the following discussion is based on the results obtained at the Becke3PW91/6-311G(d,p) level. In going from tricyclo[3.2.1.0^{2,4}]-octane, the parent hydrocarbon, to **1-opt**, the C4−C6 internuclear distance decreased from 2.446 to 1.697 Å. There were other major changes. The C2−C4, C3−C4, and C4−C5 internuclear distances increased while the C2−C3 and C5−C6 distances decreased, suggesting that double-bond character developed at these centers. Table 2 that is included as Supporting Information lists selected geometry parameters, total energies, and relative energies of **1** as a function of the C4−C6 distance. Figure 1 shows the variation of the relative energy as a function of the C4−C6 distance. When the C4−C6 distance is decreased

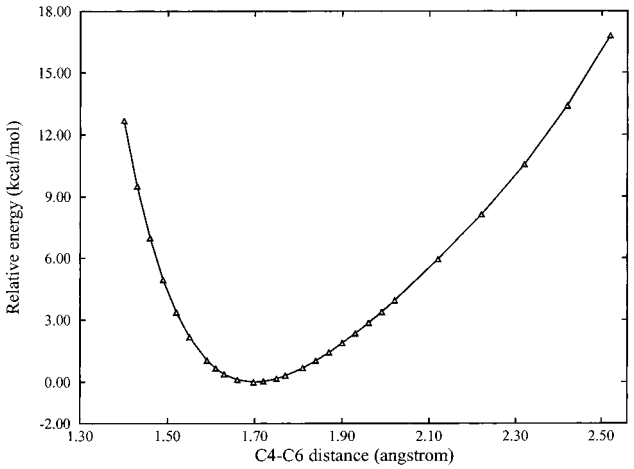

Figure 1. Plot of the relative energies (kcal mol^{-1}) of **1** as a function of the C4−C6 distance at the Becke3PW91/6-311G(d,p)//Becke3PW91/6-311G(d,p) level.

step-by-step from 1.697 to 1.40 Å and the geometry optimized, the overall change in total energy was 12.67 kcal mol^{-1}. The cyclopropyl group underwent large geometrical changes. The C2−C4 and C3−C4 distances increased by 0.229 and 0.120 Å, respectively, while the C2−C3 distance shortened by 0.037 Å. When the C4−C6 distance was increased from 1.697 to 2.320 Å, the total energy increased by 10.55 kcal mol^{-1}. At the C4−C5−C6 face, the C4−C5 distance lengthened by 0.074 Å as the C5−C6 distance shortened by 0.007 Å. In the case of the cyclopropyl group the C2−C4 and C3−C4 distances decreased by 0.107 and 0.114 Å, respectively, while the C2−C3 distance lengthened by 0.069 Å. When the C4−C6 distance reached 2.62 Å (ΔE_T =18.01 kcal mol^{-1}), **1-opt** rearranged to the isomeric cation **3-opt** that is stabilized through participation of the C5−C8 bond. In the whole range of 1.40−2.32 Å, there was no discontinuity in the total energy, and the other geometrical parameters also changed smoothly.

AIM Analysis and Delocalization Indexes. With the wave functions in hand, we analyzed the topology of charge density to gain information about the molecular structure of **1-opt**. Figure 2a is a contour plot of $\rho(\mathbf{r})$ in the C4−C5−C6 plane. A display of the gradient vector field of the charge density in the C4−C5−C6 plane is given in Figure 2b. There is no bond path between C4 and C6 even though the C4 and C6 basins appear to "impinge" on each other. This result is also seen in the 2-norbornyl cation that exhibits a T-structure regardless of whether Becke3LYP/6-31+G(d,p), MP2(full)/6-311G(d,p), or QCISD/6-31G(d,p) levels are used to obtain the wave function[9−11] even though the C1, C2, and C6 basins show this feature. Atomic interaction lines (bond paths) between C6 and C1 and C2 were found for the 2-norbornyl cation only when the internuclear distances were fixed to less than 1.65 Å. Under these circumstances ΔE_T increased by >7 kcal mol^{-1}, indicating that the species that is pentacoordinate at C6 is not the minimum on the potential energy (PE) surface.

The properties at selected bond critical points for **1-opt** are given in Table 3. The C2−C4, C3−C4, and C4−C5 bonds are weak, as reflected in the small values of electron density $\rho(\mathbf{r})$ (1.194−1.431 e Å^{-3}) and relatively small values of the Laplacian (−1.856 to −7.639 e Å^{-5}). A contour plot of the Laplacian in the C4−C5−C6 plane is shown in Figure 2c. A (3, −1) critical point in $L(\mathbf{r})$ at a value of 1.350 e Å^{-5} is located midway between C4 and C6, 0.871 Å from C4 and 0.844 Å from C6, and is labeled with an **x**. As seen from the display of

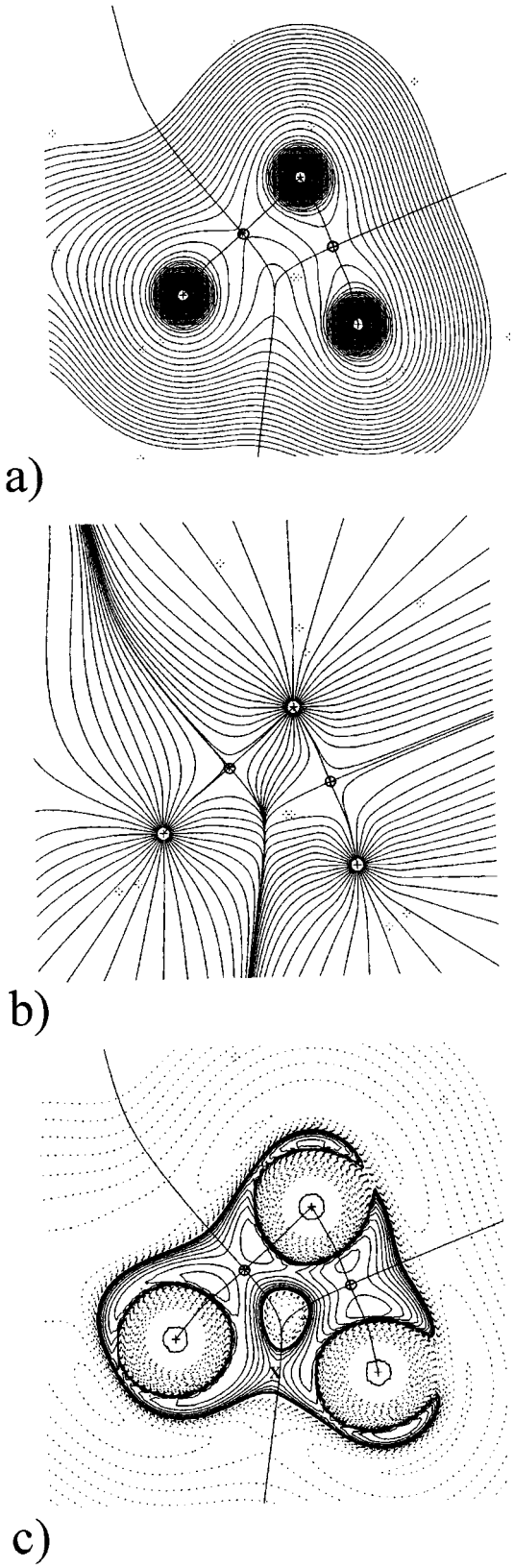

Figure 2. Display of (a) the electron density in the C4−C5−C6 plane of **1-opt**, (b) the gradient vector field of the electron density in the C4−C5−C6 plane, and (c) the Laplacian in the C4−C5−C6 plane. The bond CPs are labeled with circles. The (3,−1) CP in $L(\mathbf{r})$ is labeled with an **x**.

the 0.675 e Å^{-3} (0.1 au) contour (Figure 3a), the density itself is not particularly enlightening, providing only an indication of the molecular shape. The plot of Laplacian at an iso value of

TABLE 3: Properties at the Bond Critical Points of 1

bond	ρ (e Å^{-3})	$\nabla^2\rho$ (e Å^{-5})	ϵ^a	λ_1 (e Å^{-5})	λ_2 (e Å^{-5})
C1−C2	1.633	−13.038	0.011	−10.700	−10.604
C2−H	1.916	−23.906	0.012	−18.725	−18.508
C2−C3	1.930	−17.327	0.192	−13.640	−11.447
C2−C4	1.248	−3.446	1.464	−7.615	−3.085
C3−C4	1.194	−1.856	2.975	−7.182	−1.807
C4−H	1.916	−23.545	0.041	−18.845	−18.122
C4−C5	1.431	−7.639	0.500	−9.134	−6.097
C5−C6	1.856	−15.809	0.171	−12.869	−10.989
C6−C7	1.721	−14.532	0.016	−11.471	−11.278
C6−H	1.937	−24.533	0.026	−19.303	−18.797

[a] The ellipticity ϵ is defined as $\lambda_1/\lambda_2 - 1$.

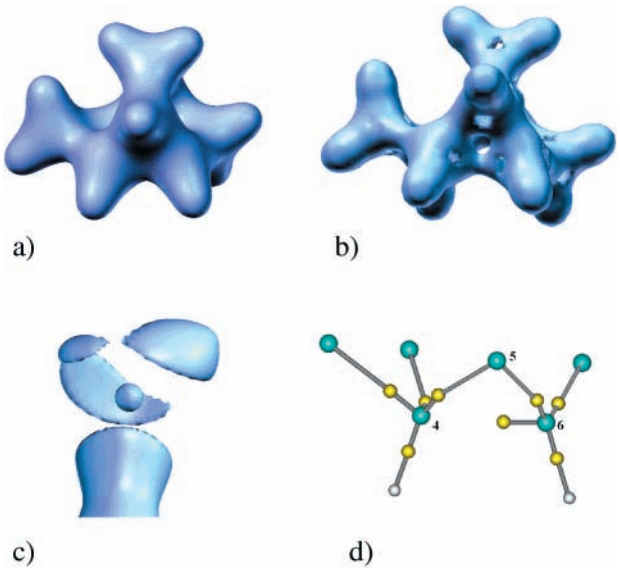

Figure 3. Display of (a) the 0.675 e Å^{-3} (0.1 au) contour of the electron density of **1-opt**, (b) the 0.0 e Å^{-5} contour of the Laplacian, (c) the 9.543 e Å^{-5} contour of the Laplacian around C4, and (d) the (3, −3) CPs (yellow spheres) of the VSCCs located around C4 and C6 (blue spheres).

0.0 e Å^{-5} displayed in Figure 3b confirmed that a saddle point might be expected between C4 and C6. Of particular interest is the fact that C4 exhibited only four VSCCs in $L(\mathbf{r})$ (the (3, −3) CPs lie 0.521−0.532 Å from the nucleus) that are directed toward C2, C3, C5, and H13, but not at C6 (compare the contours between C4−C5 and C4−C6 of Figure 2c). While most covalent bonds exhibiting bond paths have two VSCC maxima, in some cases only one maximum occurs, as, for example, in the polarized C−F bond, or none are seen, as in the case of the P−F bond in PF_3.[29] The nature of the Laplacian around C4 at an iso value of 9.543 e Å^{-5} is displayed in Figure 3c; Figure 3d shows the location of the (3, −3) CPs, indicating how VSCCs are orientated around C4 and directed toward the other atoms. The C4−VSCC−C2, C4−VSCC−C3, C4−VSCC−C3, and C4−VSCC−H angles are 153.1°, 157.9°, 158.0°, and 179.6°, respectively, indicating that the VSCCs try to keep as far as possible away from each other. It is interesting to note that C6, nominally considered to be tricoordinate, exhibits four VSCCs.

The net atomic charges of **1-opt** are listed in Table 4. For C3, C4, and C6 the net charges are +0.021, −0.211, and +0.026, respectively, at the Becke3PW91/6-311G(d,p)//Becke3PW91/6-311G(d,p) level. That C4 bears an unexpectedly large negative charge (at the HF/6-311G(d,p)//Becke3PW91/6-311G(d,p) and HF/6-311G(d,p)//HF/6-311G(d,p) levels, the charges are enormous (−0.339 and −0.323e, respectively)) is noteworthy and an indication that there is an "ionic" component to the C4−C6 interaction. We also integrated the pair density within single basins and between basins to obtain the localization and delocalization indexes λ(A,A) (LI) and δ(A,B) (DI) that are given in Table 5. The total number of electrons in **1** is 58.0, and the sum of all LIs and DIs gave a value of 57.978, indicating that the integrations were of good quality. The extent of spatial localization of electron pairs is determined by the corresponding property of the Fermi hole density. Integration of the pair density yields the Fermi correlation contained in a single basin F(A,A) (its magnitude is the localization index λ(A,A)) and F(A,B), the correlation shared between two basins. The quanity F(A,B) is a measure of the extent to which electrons of either spin referenced to atom A are delocalized into atom B with a corresponding definition of F(B,A). Thus F(A,B) = F(B,A) and their sum $|F(A,B)| + |F(B,A)| = \delta(A,B)$ that is termed the delocalization index is a measure of the total Fermi correlation shared between the atoms (basins). According to the integration property of the Fermi hole of an electron, the atomic and interatomic Fermi correlations sum to $-N$, the total number of electrons of a molecule. Correspondingly, the sum of the localization and delocalization indexes gives N while providing a quantitative measure of how the N electrons are localized within the atomic basins and delocalized between them. Each atomic population $\bar{N}$(A) is given by the expression $\bar{N}(A) = |F(A,A)| + \sum_{B\neq A}\delta(A,B)/2$. The localization index $|F(A,A)|$ has a limiting value of $\bar{N}$(A), corresponding to complete localization of the $\bar{N}$(A) electrons to the basin of atom A. The percent localization (PL) given as $|F(A,A)|/\bar{N}(A) \times 100$ is a measure of the electron localization and provides information about the ionic character of a bond; if the value is in the region of 100%, the population is −1.0 or +1.0, for example, bonding is purely ionic. As seen in Table 5, the PLs for C2, C3, C4, C5, and C6 of **1** that lie in the region of 66% do not differ significantly from the PLs of the parent hydrocarbon and they are virtually

TABLE 4: Net Charge on Carbon Atoms as a Function of the C4−C6 Distance and BeH Substitution[a]

	C4−C6 distance/Å					
	1.40	1.55	1.62	1.697 (1.692)[b,c] opt	2.32	4,5-$(BeH)_2$ opt
C1	0.029	0.038	0.040	0.043 (0.123) [0.118]	−0.051	0.043
C2	0.015	0.012	0.013	0.011 (0.041) [0.037]	−0.019	−0.0003
C3	0.007	0.024	0.023	0.021 (0.104) [0.093]	−0.005	0.017
C4	−0.205	−0.221	−0.219	−0.211 (−0.323) [−0.339]	−0.089	−0.855
C5	0.006	0.006	0.007	0.008 (0.029) [0.065]	0.005	−0.673
C6	0.048	0.036	0.031	0.026 (0.075) [0.023]	0.026	0.019
C7	0.032	0.032	0.032	0.030 (0.157) [0.146]	0.025	0.028
C8	0.023	0.019	0.019	0.018 (0.135) [0.124]	−0.016	0.006

[a] Unless otherwise noted, the calculation level is Becke3PW91/6-311G(d,p)//Becke3PW91/6-311G(d,p). [b] The values in parentheses were obtained with the wave function obtained at the HF/6-311G(d,p)//HF/6-311G(d,p) level. The values in square brackets were obtained with the wave function obtained at the HF/6-311G(d,p)//Becke3PW91/6-311G(d,p) level. [c] The corresponding values for C1 to C8 for the parent hydrocarbon tricyclo[3.2.1.0^{2,4}]octane are 0.046, −0.046, −0.051, −0.046, 0.046, 0.014, 0.014 and 0.003, respectively.

TABLE 5: Localization Indexes $|F(A,A)|$ of Selected Atomic Basins and Delocalization Indexes $\delta(A,B)$ of Selected Pairs of Basins[a]

	A	$\|F(A,A)\|$	%[b]	A,B	$\delta(A,B)$	C4−C6	A	$\|F(A,A)\|$	%[b]	A,B	$\delta(A,B)$
opt[c]	C1	3.864	64.9	C1,C2	0.944 (0.937)[d]	1.55	C1	3.869	64.9	C1,C2	0.950
	C2	3.918	65.4	C2,C3	1.112 (1.108)		C2	3.929	65.6	C2,C3	1.1670
	C3	3.983	66.6	C2,C4	0.745 (0.742)		C3	3.989	66.8	C2,C4	0.660
	C4	4.105	66.1	C3,C4	0.733 (0.731)		C4	4.105	66.0	C3,C4	0.673
	C5	3.913	65.3	C4,C5	0.860 (0.862)		C5	3.924	65.5	C4,C5	0.875
	C6	3.945	66.1	C4,C6	0.634 (0.626)		C6	3.903	65.4	C4,C6	0.784
	H(C4)	0.333	38.6	C5,C6	1.037 (1.036)		H(C4)	0.330	38.4	C5,C6	0.998
				C4,H	0.911 (0.935)					C4,H	0.905
HF opt[e]	C1	3.801	64.7	C1,C2	0.937	1.62	C1	3.867	64.9	C1,C2	0.947
	C2	3.908	65.6	C2,C3	1.124		C2	3.923	65.5	C2,C3	1.138
	C3	3.909	66.3	C2,C4	0.717		C3	3.986	66.7	C2,C4	0.703
	C4	4.220	66.8	C3,C4	0.720		C4	4.106	66.0	C3,C4	0.703
	C5	3.858	65.1	C4,C5	0.869		C5	3.918	65.4	C4,C5	0.867
	C6	3.967	66.4	C4,C6	0.636		C6	3.923	65.7	C4,C6	0.711
	H(C4)	0.357	39.9	C5,C6	1.036		H(C4)	0.330	38,0.4	C5,C6	1.018
				C4,H	0.939					C4,H	0.908
4,5-$(BeH)_2$	C1	3.860	64.8	C1,C2	0.959	2.32	C1	3.856	64.8	C1,C2	0.943
	C2	3.919	65.3	C2,C3	1.122		C2	3.933	65.4	C2,C3	0.984
	C3	3.969	66.4	C2,C4	0.740		C3	3.977	66.2	C2,C4	0.946
	C4	4.925	71.9	C3,C4	0.768		C4	4.018	66.0	C3,C4	0.928
	C5	4.803	72.0	C4,C5	0.912		C5	3.908	65.2	C4,C5	0.821
	C6	3.916	65.5	C4,C6	0.727		C6	4.053	67.9	C4,C6	0.189
	Be13	2.01	85.9	C5,C6	1.068		H(C4)	0.366	40.5	C5,C6	1.122
	Be14	2.01	86.1	C4,Be13	0.252					C4,H	0.936
	H20	1.552	86.9	C5,Be14	0.259						
	H21	1.567	87.3	Be13,H	0.351						
				Be14,H	0.346						

[a] Unless otherwise noted, the calculation level is Becke3PW91/6-311G(d,p)//Becke3PW91/6-311G(d,p). [b] The percent localization, $|F(A,A)|/\bar{N}(A) \times 100$. [c] For the parent hydrocarbon tricyclo[3.2.1.0^{2,4}]octane at the Becke3PW91/6-311G(d,p)//Becke3PW91/6-311G(d,p) level, the localization index and the percent localization at C4, C6, and H(C4) are 3.945 and 65.3%, 3.913 and 65.4%, and 0.428 and 43.5%, respectively. The delocalization index between C4 and C6 is 0.057. [d] The values in parentheses were obtained with the wave function obtained at the HF/6-311G(d,p)//Becke3PW91/6-311G(d,p) level. [e] The values were obtained with the wave function obtained at the HF/6-311G(d,p)//HF/6-311G(d,p) level.

identical at the DFT and HF levels. There was no significant dependence of the PLs on the C4−C6 distance.

To ascertain the effect of substituents on the molecular structure of **1**, we replaced the hydrogens of **1** with a range of substituents including Li, BeH, BH_2, CH_3, and SiH_3. Only when Li and BeH groups replace hydrogens on C4 and C5 (the C4−C6 distances are 1.617 and 1.660 Å) was a bond path found between C4 and C6 with five VSCCs located around C4. As was seen in **1-opt** when the C4−C6 distance was fixed at 1.62 Å, the bond path dwells away from atomic connection line and the bond CP (**o**) is very close to the ring CP (*) (Figure 6a), an indication that these CPs are close to the point of anihilation. Moreover, the electron densities at the bond and the ring CPs are equal (1.221 e Å^{-3}), and the Laplacian has values of −0.868 and 1.078 e Å^{-5}, respectively. Only when the hydrogens at C4 and C5 are replaced with the electropositive substituents BeH and Li (data not shown for the latter) does the ionicity of the bonding to C4 and C5 increase and do these carbon atoms possess large negative charges (Table 4).

According to theory, the 1,2-DI is unity when a single pair of electrons is shared equally between adjacent atoms of a homonuclear bond.[16,17] The 1,3-DI between the C4 and C6 basins is surprisingly large (0.634), but smaller than the 1,2-DIs between C2−C4 (0.745), C3−C4 (0.733), and C4−C5 (0.860), which, unlike C4 and C5, are connected by bond paths. In the cases **1** with the C4−C6 distance fixed at 1.62 Å and **1** substituted with BeH and Li groups at C4 and C5, where bond paths connected C4 and C6, the 1,3 DIs increased to 0.711 and 0.727, respectively. For the parent hydrocarbon and **1** with the C4−C6 distance fixed at 2.32 Å the C4 and C6 DIs are 0.057 and 0.189, respectively, indicating that there is little or no homoconjugative interaction between C4 and C6 in these cases. These results suggest that a 1,3 DI of greater than 0.7 and an internuclear distance in the range 1.6−1.65 Å are the key requirements for the existence of pentacoordinate carbons in polycyclic carbocations. The DIs between C4 and other atomic basins of **1** sum to 4.214, roughly obeying the octet rule (four pairs, eight electrons). The DIs of C2−C3 and C5−C6 are greater than 1.00 (1.037 and 1.112) in keeping with the fact that these bonds have double bond character. To relate the DIs of a classical cation that is considered to be stabilized by hyperconjugation, we studied the C_{3v} *tert*-butyl cation (**4-opt)** at the Becke3PW91/6-311G(d,p) level. The H6−C2, H5−C2, and H7−C2 1,3-DIs are 0.101, 0.052, and 0.052, respectively; the C−H distances for these two different types of hydrogens are 2.049 and 2.141 Å. That hyperconjugation reduces the degree of covalent bonding in the C−H bond that is coplanar with the vacant p orbital is seen in the fact that the C1−H6 DI (0.865) is less than the C1−H5 and C1−H7 DIs (0.921). For the parent hydrocarbon, 2-methylpropane, the 1,3-DIs between C2 and the methyl hydrogens (the distances are 2.181 and 2.174 Å) are 0.0393, 0.0393, and 0.041, respectively, and the DIs for the C−H bonds are 0.958, 0.958, and 0.950. We take these as standard values for the isobutyl system. Thus, the 1,3-DIs for the *tert*-butyl cation are only marginally larger than the values found for the parent hydrocarbon and it is clear that the internuclear distance/bond angle may be one of the factors that determine the magnitude of the DI. It is also interesting to note that the C1−C2 DI is 1.111, confirming, as expected, that there is double bond character (the C−C distance is 1.460 Å) in the three C−C bonds of **4-opt**. For the parent hydrocarbon, the DI for the C−C bond (1.529 Å) is 0.981. The results obtained for **4-opt** are in keeping with the generally accepted view that hyperconjugation is maximized when a C−H bond is aligned

coplanar with an adjacent vacant p orbital on carbon. That the C−Be and Be−H bonds of 4,5-$(BeH)_2$-**1** have a large degree of ionicity is seen in their DIs: 0.259 and 0.252 for the former and 0.346 and 0.351 for the latter.

ELF Analysis. Our ELF study on the 2-norbornyl cation[12] at the Becke3LYP/cc-pVTZ level revealed that a single trisynaptic basin connected C6 to C1 and C2 in the optimized geometry, while disynaptic basins linked C1−C6 and C2−C6 at the MP2(full)/6-311G(d,p), Becke3PW91/cc-pVTZ, and QCISD/6-31G(d,p) levels. While the C6−C1(C2) distance was 1.889 Å at Becke3LYP it ranged between 1.826 and 1.846 Å at the MP2(full), QCISD, and Becke3PW91 levels. Yet small increases in the C6−C1(2) distances resulted in C6 being disconnected from C1 and C2 with ΔE_T ranging from 0.14 to 0.50 kcal mol^{-1} depending on the level of theory used. No discontinuity was seen in E_T when these disconnections occurred. This study established that small changes in molecular geometry affect the outcome of ELF analyses so attention was paid to that possibility. The integration of the one-electron density $\rho(\mathbf{r})$ and of the pair function $\pi(\mathbf{r}_1,\mathbf{r}_2)$ over the volume Ω of one basin provides the population $\bar{N}(\Omega)$ of a basin and its variance σ^2, the latter being a measure of the contribution from other basins to $\bar{N}(\Omega)$. The relative fluctuation $\lambda = \sigma^2/\bar{N}(\Omega)$ provides an indication of the delocalization within that basin, while the percent contribution fluctuations (%) give a quantitative measure of the contributions of other basins to the variance σ^2.[19]

The C−C valence basins of **1-opt** can basically be divided into three groups. The first group that includes V(C2,C4), V(C3,C4), and V(C4,C6) has small populations (0.83−1.22e), small volumes (10.28−12.60 Å^3), and large fluctuations (0.68−0.76). They are also differentiated by the fact that the attractors, the (3, −3) CPs, are located closer to C4 (0.777−0.793 Å) than the other carbon atoms (0.883−1.002 Å) and they do not lie on the geometric connection line between the atoms. The C4−V(C4,C)−C angles range between 144.8° and 153.6°. The second group includes V(C5,C6) and V(C2,C3) that have a teardrop shape at the 0.75 contour (Figure 4c(4d) and Figure 4e(4f) in yellow) in keeping with the fact that these bonds exhibit partial double bond character; ethene exhibits a dumbbell-shaped C,C valence basin at this contour value. The V(C2,C3) CP is equidistant from C2 and C3, while the one associated with V(C5,C6) is slightly closer to C6 (0.743 Å) than C5 (0.791 Å). The remaining basins that are pill-shaped (in green) fall in the third group. The CPs lie on the geometric atomic connection line between the carbon atoms and their basin populations are in the region 2.0, showing the normal covalent C−C bonds within the ELF formalism. V(C4,C5) exhibits properties (a population of 1.64e, a volume 20.4 Å^3, and a fluctuation of 0.60) that lie roughly midway between those of these basins and the first group. The disynaptic basin V(C4,C6) between C4 and C6, shown in red in Figure 4a,c) has an ELF value of 0.810 at its (3, −3) CP (attractor). It has a small population of only 0.83e, a large fluctuation (0.76), and its (3, −3) CP (yellow) is located 0.771 Å from C4 and 1.000 Å from C6, as seen in Figure 4b; the C4−V(C4,C6)−C6 angle is 144.8°. As seen in Table 6, seven valence basins communicate (percent contributions of less than 4% are arbitrarily excluded) with the C4−C6 basin of **1-opt**.

Silvi and co-workers have demonstrated that localization reduction tree diagrams are useful in analyzing the hierarchy of valence basins.[30] The tree diagram for **1-opt** shows that it is possible to divide the valence shell of C4 (see Figure 4a) roughly into three main regions (a) V(C4,H), (b) the union of the V(C3,C4) and V(C4,C5) basins and (c) the union of V(C2,C4) and V(C4,C6) basins. The bifurcation values for the union of the V(C3,C4) and V(C4,C5) basins and the union of V(C2,C4) and V(C4,C6) are 0.771 and 0.786, and so they still share separate matrices at an ELF value of 0.75, as seen in Figure 4a. Nevertheless, the ELF values at the attractors of the four disynaptic basins V(C3,C4), V(C4,C5), V(C2,C4), and V(C4,C6) are 0.856, 0.915, 0.867, and 0.810, respectively. Considering

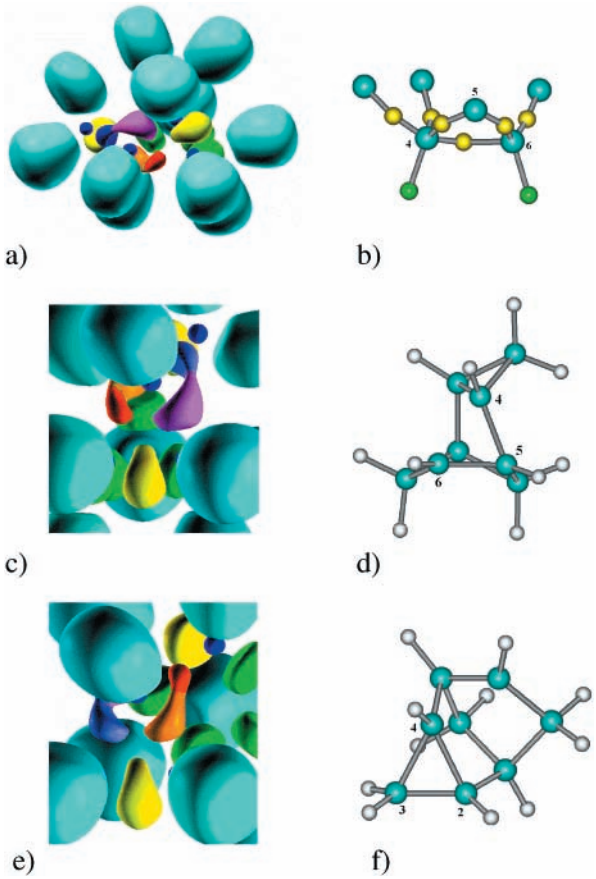

Figure 4. Display of (a) the 0.75 contour of the ELF basins of **1-opt** with the following color coding: C,H basins, light blue; C3,C4 basin, purple; C4,C2 basin, orange; C4,C5 basin, magenta; C4,C6 basin, red; C2,C3 and C5,C6 basins, yellow; C1,C2, C6,C7, and C7,C1 basins, green; carbon cores, small purple spheres, (b) the location of the (3, −3) CPs (attractors) in ELF around C4 and C6, (c) the ELF basins (0.75 contour) viewed perpendicular to the C4−C5−C6 plane, (d) **1-opt** viewed perpendicular to the C4−C5−C6 plane, (e) the ELF basins (0.75 contour) viewed perpendicular to the C2−C3−C4 plane, (f) **1-opt** viewed perpendicular to the C2−C3−C4 plane.

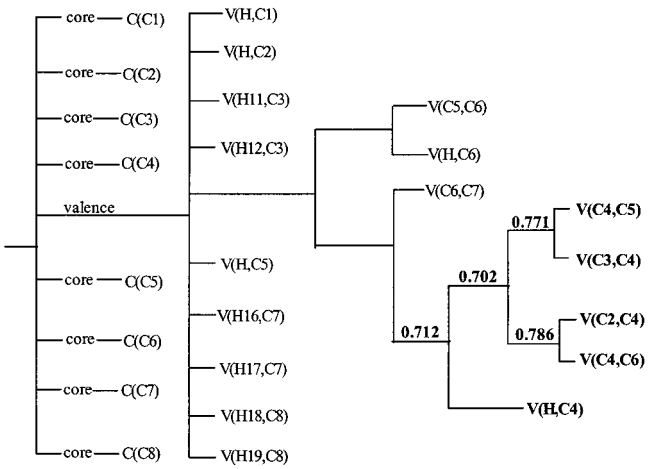

TABLE 6: Population ($\bar{N}$), Variance (σ^2), Relative Fluctuation (λ), Volume (Ω, Bohr^3), ELF Values (η) at (3, −3) Critical Points and Contribution of Other Basins to the Variance (σ^2) of Selected Basins of 1

basin	$\bar{N}$	σ^2	λ	Ω	h	contribution analysis (%)
V(C1,C2)	1.93	1.02	0.53	19.52	0.957	15.0 V(H,C1); 14.7V(H,C2); 13.1V(C2,C3); 8.5V(C2,C4); 5.9C(C2); 4.8C(C1)
V(C2,H)	2.12	0.67	0.32	72.69	1.000	24.7V(C2,C3); 22.8V(C1,C2); 15.3V(C2,C4); 11.2C(C2); 3.0V(H12,C3); 2.5V(H,C4); 2.4V(H11,C3);
V(C2,C3)	2.09	1.06	0.51	32.33	0.949	15.7V(H11,C3); 15.6V(H,C2); 15.5V(H12,C3); 10.1V(C4.C6); 9.3V(C3,C4); 5.9C(C2); 5.9C(C3)
V(C2,C4)	1.22	0.82	0.68	12.60	0.867	13.0V(C2,C3); 12.3V(H,C2); 11.7V(H,C4); 11.3V(C4,C6); 11.3V(C3,C4); 10.4V(C1,C2); 4.4C(C4); 3.0C(C2);
V(C3,C4)	1.04	0.74	0.71	11.68	0.856	14.0V(H,C4); 13.8V(C4,C5); 13.5V(C2,C3); 12.7V(C2,C4); 12.0V(H11,C3); 12.0V(H12,C3); 4.0C(C4); 3.27 V(C4,C6); 3.0C(C3)
V(C4,H)	2.16	0.71	0.33	74.83	1.000	18.9V(C4.C5); 14.5V(C3,C4); 13.7V(C2,C4); 13.0V(C4,C6); 10.9C(C4)
V(C4,C5)	1.64	0.98	0.60	20.41	0.915	13.7V(H,C4); 13.5V(H,C5); 13.0V(C5,C6); 10.9VC5,C8); 10.3V(C3,C4); 8.8V(C4,C6); 5.8V(C2,C4); 5.2C(C4); 3.8C(C5)
V(C4,C6)	0.83	0.63	0.76	10.28	0.810	14.9V(C2,C4); 14.7V(H,C4); 13.7V(C4,C5); 12.0V(C5,C6); 11.0V(H,C6); 9.4V(C6,C7); 3.8V(C3,C4); 3.7C(C4); 2.4C(C6)
V(C5,C6)	2.02	1.06	0.52	26.12	0.947	15.5V(H,C6); 15.3V(H,C5); 12.8V(C6,C7); 12.4V(C5,C8); 12.0V(C4.C5); 7.1V(C4,C6); 5.9C(C6); 5.4C(C5)
V(C6,C7)	1.99	1.03	0.52	20.19	0.958	15.6V(H,C6); 14.9V(H16,C7); 14.9V(H17,C7); 13.1V(C5,C6); 11.7V(C1,C7); 6.1C(C6); 5.7V(C4,C6); 5.0C(C7)
V(C6,H)	2.14	0.66	0.31	78.54	1.000	25.2V(C5,C6); 24.5V(C6,C7); 11.7C(C6); 10.6V(C4,C6)

that these four basins lose their union with V(C4,H) at an ELF value of 0.712 and V(C4,C5) and V(C4,C6) have a bifurcation value of 0.702, the V(C2,C4) and V(C4,C6) union (the bifurcation value is 0.786 and is close to the value of the V(C4,-C6) attractor (0.810)) can be considered "chemically significant" in this ELF analysis. In fact, the V(C2,C4) and V(C4,C6) disynaptic basins merged into a single trisynaptic basin involving C2, C4, and C6 when the C4−C6 distance was increased to 1.78 Å. Yet the energy of **1** only increased by 0.38 kcal mol^{-1}. At a C4−C6 distance of 1.87 Å the connection to C6 was lost and the trisynaptic basin was reduced to a disynaptic basin between C2 and C4. In going from **1-opt** to the 1.87 Å geometry, the total increase in energy was 1.42 kcal mol^{-1}! At the Becke3LYP/6-311G(d,p) level the disynaptic V(C4,C6) basin merged with V(C2,C4) to form a trisynaptic basin when the C4−C6 distance was 1.78 Å (ΔE_T was +0.13 kcal mol^{-1}) and the trisynaptic basin collapsed into V(C2,C4) at 1.87 Å. ΔE_T was 0.76 kcal mol^{-1} relative to **1-opt** at the Becke3LYP/6-311G(d,p) level. We observed this dependence on functional while studying the 2-norbornyl cation.[10] In our view, the V(C4,-C6) disynaptic basin does not identify a bonifide covalent bonding interaction. On the whole, the C4,C6 interaction appears to be ionic in character, in accord with the fact that the V(C4,-C6) basin is closer to C4 (the attractor is 0.777 Å from C4 and 1.002 Å from C6) and the C(C4)−V(C4,C6)−C(C6) angle of 144.8° deviates significantly from the geometric interatomic line.

In going from **1-opt** to the 1.62 Å geometry where C4 and C6 are connected with a bond path, the population of V(C4,-C6) increased from 0.83 to 1.13e, the variance increased from 0.63 to 0.79, the volume increased from 10.28 to 13.53 bohr^3, and the fluctuation decreased from 0.76 to 0.70. These data and the fact that the ELF value at the (3, −3) CP increased from 0.81 to 0.85 indicate a sizable buildup of electronic charge between C4 and C6. Yet, in going from **1-opt** to the 1.62 geometry the energy change was only 0.51 kcal mol^{-1}. V(C4,-C6) is disynaptic and it has significant percent contributions to the fluctuation only from C4 and C6 core basins.

In general, homeomorphism is observed between the number and spatial arrangement of the maxima displayed by ELF and the VSCCs of $L(\mathbf{r})$.[31] This was not the case in the **1-opt**. One disynaptic basin was located between C4 and C6 but nearer to C4 than C6, while a VSCC was located within the valence shell of C6 directed to C4. In our case the ELF disynaptic basins around C4 correlate with the (3, −1) critical points in $L(\mathbf{r})$ but not the with theVSCCs (3, −3 CPs) of $L(\mathbf{r})$ around C4. Since $L(\mathbf{r})$ exhibits a homeomorphism with the Laplacian of the conditional same-spin pair density, it is the topology of $L(\mathbf{r})$ rather than that of ELF that is to be used in cases where the two fields differ in their predictions.[15,31]

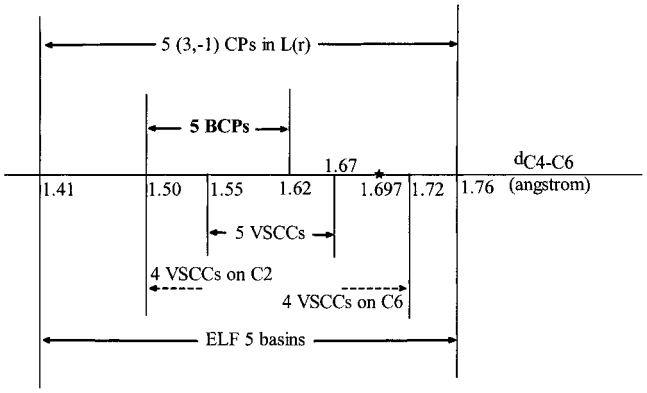

Figure 5. Schematic diagram of the variation of selected critical points as a function of the C4−C6 distance of **1**.

In summary, all carbon atoms of **1-opt** except C6 are connected by four bond paths and only four valence shell (3, −3) CPs are found in the Laplacian. Yet, a (3, −1) critical point with a close-to-zero value is found between C4 and C6, showing that there are five (3, −1) CPs in the Laplacian between C4 and five other atoms. In line with this result is the finding that there are five disynaptic basins in ELF that connect C4 and other five atoms. Since C4 has four bond paths and only four valence shell (3, −3) CPs are found in Laplacian, we consider **1-opt** to be best described as a classical cation that has a high degree of delocalization involving C4 and C6; it's a σ/π no-bond homoconjugated species.

Nature of AIM and ELF Critical Points as a Function of the C4−C6 Distance. The nature of the critical points around C4 as a function of C4−C6 distance are summarized graphically in Figure 5. There are five bond paths to C4 when the C4−C6 distance ranged from 1.5 to 1.62 Å, while five VSCCs were located around C4 when the C4−C6 distance ranged between 1.55 and 1.67 Å. The nominal cationic center C6 possessed four VSCCs up to a distance of 1.72 Å and then the one directed at C4 was lost. When the C4−C6 distance was reduced to less than 1.50 Å, C2 lost one VSCC and the C2−C4 bond path disappeared. The (3, −1) CPs in $L(\mathbf{r})$ located midway between

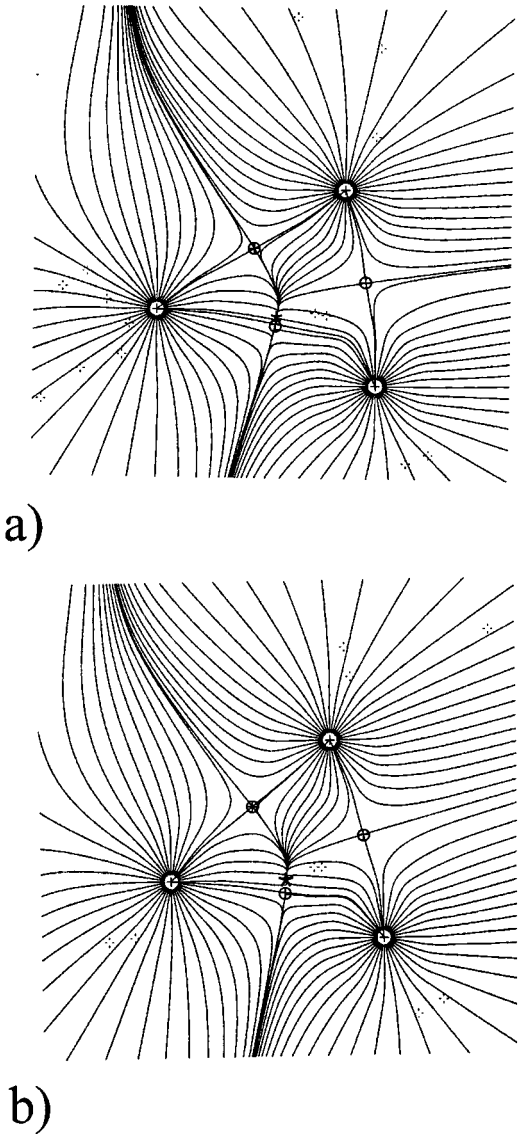

Figure 6. Display of (a) the gradient vector field of the electron density of **1** in the C4−C5−C6 plane when C4−C6 distance is 1.62 Å, and (b) the gradient vector field of the electron density in the C4−C5−C6 plane of **1** substituted with BeH groups at C4 and C5. The bond CPs are labeled with circles. The (3, +3) ring CPs are labeled with an asterisk.

the nuclei and ELF basins have common features and both are not very sensitive to the changes of C4−C6 distance. As seen from the gradient vector field of density in the C4−C5−C6 plane, a curved bond path appears between C4 and C6 at a C4−C6 distance of 1.62 Å (Figure 6a). At this point the C4−C6 DI is 0.711. This result is reminiscent of what we found for the 2-norbornyl cation. The densities at the bond critical point and at the ring critical point are virtually identical (1.81 and 1.80 e $Å^{-3}$, respectively). The Laplacian at these two points is close to zero. From 1.697 to 1.620 Å, the total energy only increased by 0.51 kcal mol^{-1}. At this point the covalent bonding between C4 and C6 is marginal. While there is a bond path and five VSCCs are found around C4, the bond path dwells away from atomic connection line and the bond CP is very close to the ring CP, an indication that these CPs are close to the point of anhilation as was seen for 4,5-$(BeH)_2$-**1** (Figure 6b). The properties at the selected bond critical points and the properties of the selected ELF basins are listed in Table 7 and Table 8 that are included as Supporting Information.

Conclusions

The 6-tricyclo[3.2.1.$0^{2,4}$]octyl cation is a classical species that exhibits a σ/π no-bond homoconjugation between C4 and C6. It has no pentacoordinated carbon atoms and the bonding may have an ionic component. Only when the C4−C6 distance is fixed in the range 1.50−1.62 Å does it become a pentacoordinate (nonclassical) species in which C4 is connected to C2, C3, C5, C6, and H13 with bond paths. For polycyclic species such as **1**, it appears that a delocalization index of approximately 0.7 and an internuclear distance of 1.6 Å are required for a bond path to materialize between remote carbons. The 6-tricyclo-[3.2.1.$0^{2,4}$]octyl cations substituted with Li and BeH groups at C4 and C5 are pentacoordinate species.

Acknowledgment. We are indebted to Professor Richard Bader for his stimulating discussions. We thank Dr. Stéphane Noury, Ms. Maggie Austen, and Mr. Chérif Matta for many helpful discussions. We greatly acknowledge the grant of CPU time on a CRAY T90 vector computer at the NIC at the Research Center Jülich and the usage of the SGI computing installation in the Geochemistry Labs at McMaster funded by the Natural Sciences and Engineering Research Council of Canada (NSERC). We also acknowledge a grant of CPU time on a SGI Origin 2001 at the Universite de Montreal under the auspices of the Reseau de Quebecois de Calcul Haute Performance (RQCHP). We thank NSERC for financial support.

Supporting Information Available: Table 2 giving selected geometry parameters, total energies, and relative energies of **1** as a function of the C4−C6 distance and Tables 7 and 8 listing properties at the selected bond critical points and the properties of the selected ELF basins. This material is available free of charge via the Internet at http://pubs.acs.org.

References and Notes

(1) (a) Wiberg, K. B.; Wenzinger, G. R. *J. Org. Chem.* **1965**, *30*, 2278. (b) Colter, A. K.; Musso, R. C. *J. Org. Chem.* **1965**, *30*, 2462.
(2) Berson, J. A.; Bergman, R. G.; Clarke, G. M.; Wege, D. *J. Am. Chem. Soc*. **1969**, *91*, 5601.
(3) Werstiuk, N. H.; Wang, Y. G. *ARKIVOC*, in press.
(4) Haywood-Farmer, J. *Chem. Rev*. **1974**, *74*, 315.
(5) Cremer, D.; Childs, R. L.; Kraka, E. In *The Chemistry of the cyclopropyl group*; Rappoport, Z., Ed.; John Wiley & Sons Ltd: New York, 1995; Vol. 2, pp 339−410.
(6) Cecchi, P.; Pizzabiocca, A.; Renzi, G.; Grandinetti, F.; Sparapani, C.; Buzek, P.; Schleyer, P von R.; Speranza, M. *J. Am. Chem. Soc.* **1993**, *115*, 10338.
(7) Szabó, K. J.; Cremer, D. *J. Org. Chem*. **1995**, *60*, 2257.
(8) Werstiuk, N. H.; Muchall, H. M. *J. Mol. Struct. (THEOCHEM)* **1999**, *463*, 225.
(9) Muchall, H. M.; Werstiuk, N. H. *J. Phys. Chem. A* **1999**, *103*, 6599.
(10) Werstiuk, N. H.; Muchall, H. M. *J. Phys. Chem. A* **2000**, *104*, 2054.
(11) Werstiuk, N. H.; Muchall, H. M.; Noury, S. *J. Phys. Chem. A* **2000**, *104*, 11601.
(12) Bader, R. F. W. *Atoms in Molecules-A Quantum Theory*; Oxford University Press: Oxford, U.K., 1990.
(13) Bader, R. F. W. *J. Phys. Chem. A* **1998**, *102*, 731.
(14) Fradera, X.; Austen, M. A.; Bader, R. F. W. *J. Phys. Chem. A* **1999**, *103*, 304.
(15) Molina, J. M.; Dobado, J. A.; Heard, G. L.; Bader, R. F. W.; Sundberg, M. R. *Theo. Chem. Acc*. **2001**, *105*, 365.
(16) Bader, R. F. W.; Matta, C. F. A SEA CHANGE.
(17) Becke, A. D.; Edgecombe, K. E. *J. Chem. Phys.* **1990**, *92*, 5397.
(18) Silvi, B.; Savin, A. *Nature* **1994**, *371*, 683.
(19) Noury, S.; Colonna, A.; Savin, A.; Silvi, B. *J. Mol. Struct. (THEOCHEM)* **1998**, *450*, 59.
(20) Savin, A.; Silvi, B.; Colonna, F. *Can. J. Chem*. **1996**, *74*, 1088.
(21) Savin, A.; Nesper, R.; Wengert, S.; Fassler, T. F. *Angew. Chem., Int. Ed. Engl.* **1997**, *36*, 1809.
(22) Frisch, M. J.; Trucks, G. W.; Schlegel, H. B.; Gill, P. M. W.; Johnson, B. G.; Robb, M. A.; Cheeseman, J. R.; Keith, T.; Petersson, G. A.; Montgomery, J. A.; Raghavachari, K.; Al-Laham, M. A.; Zakrzewski, V. G.; Ortiz, J. V.; Foresman, J. B.; Peng, C. Y.; Ayala, P. Y.; Chen, W.; Wong, M. W.; Andres, J. L.; Replogle, E. S.; Gomperts, R.; Martin, R. L.;

Fox, D. J.; Fox, D. J.; Binkley, J. S.; Defrees, D. J.; Baker, J.; Stewart, J. P.; Head-Gordon, M.; Gonzalez, C.; Pople, J. A. *Gaussian 94*, Revision B.3; Gaussian, Inc.: Pittsburgh, PA, 1995.

(23) Frisch, M. J.; Trucks, G. W.; Schlegel, H. B.; Scuseria, G. E.; Robb, M. A.; Cheeseman, J. R.; Zakrzewski, V. G.; Montgomery, J. A.; Stratmann, R. E.; Burant, J. C.; Dapprich, S.; Millam, J. M.; Daniels, A. D.; Kudin, K. N.; Strain, M. C.; Farkas, O.; Tomasi, J.; Barone, V.; Cossi, M.; Cammi, R.; Mennucci, B.; Pomelli, C.; Adamo, C.; Clifford, S.; Ochterski, J.; Petersson, G. A.; Ayala, P. Y.; Cui, Q.; Morokuma, K.; Malick, D. K.; Rabuck, A. D.; Raghavachari, K.; Foresman, J. B.; Cioslowski, J.; Ortiz, J. V.; Stefanov, B. B.; Liu, G.; Liashenko, A.; Piskorz, P.; Komaromi, I.; Gomperts, R.; Martin, R. L.; Fox, D. J.; Keith, T.; Al-Laham, M. A.; Peng, C. Y.; Nanayakkara, A.; Gonzalez, C.; Challacombe, M.; Gill, P. M. W.; Johnson, B. G.; Chen, W.; Wong, M. W.; Andres, J. L.; Head-Gordon, M.; Replogle, E. S.; Pople, J. A. *Gaussian 98*, Revision A.1; Gaussian, Inc.: Pittsburgh, PA, 1998.

(24) Biegler-Konig, F. W.; Bader, R. F. W.; Tang, T.-H. *J. Comput. Chem.* **1982**, *3*, 317.

(25) Matta, C. F. *AIMDELOC 01*, Quantum Chemistry Program Exchange; Indiana University: Bloomington, IN, 2001; QCPE0802.

(26) Noury, S.; Krokidis, X.; Fuster, F.; Silvi, B. *TopMod* 1997.

(27) Noury, S.; Krokidis, X.; Fuster, F.; Silvi. B. *Compu., Chem*. **1999**, *23*, 597.

(28) Pepke, E.; Murray, J.; Lyons, J.; Hwu, T.-Y. *SciAn*, Version 1.21 Alpha; Supercomputer Computations Research Institute, Florida State University: Tallahassee, FL.

(29) MacDougall, P. J. The Laplacian of The Electronic Charge Distribution. Ph.D. Thesis, McMaster University, 1989.

(30) Calatayud, M.; Andres, J.; Beltran, A.; Silvi, B. *Theor. Chem. Acc.* **2001**, *105*, 299.

(31) Bader, R. F. W.; Johnson, S.; Tang, T.-H.; Popelier, P. L. A. *J. Phys. Chem*. **1996**, *100*, 15398.